

Electron localization in the insulating state: Application to crystalline semiconductors

Claudia Sgiarovello, Maria Peressi, and Raffaele Resta

Istituto Nazionale di Fisica della Materia (INFM) and Dipartimento di Fisica Teorica,

Università di Trieste, Strada Costiera 11, I-34014 Trieste, Italy¹

and Institut Romand de Recherche Numérique en Physique des Matériaux (IRRMA),

CH-1015 Lausanne, Switzerland²

Abstract

The insulating state of matter is characterized by the excitation spectrum, but also by qualitative features of the electronic ground state. The insulating ground wavefunction in fact: (i) sustains macroscopic polarization, and (ii) is *localized*. We describe both properties using essentially the same formalism, based on Berry phases and related quantities, and specializing to the case of a crystalline system of independent electrons. We measure localization in different materials by means of a “localization tensor”: we analyze its properties, and we actually compute it from first principles for several tetrahedrally coordinated semiconductors. We discuss the trends in our calculated quantity, and we relate our findings to related recent work. We also address orbitals (“hermaphrodite orbitals”) which are optimally localized (Wannier-like) in a given direction, and delocalized (Bloch-like) in the two orthogonal directions: we prove numerically that their localization is exponential.

I. INTRODUCTION

A nonmetal is distinguished from a metal by its vanishing conductivity at low temperature and low frequency: we use here the term “insulator” to include any nonmetal, like the semiconducting materials which are the case studies actually addressed in this work.

Within classical physics, the qualitative difference between an insulator and a metal is attributed to the nature of the electronic charge: either “bound” (Lorentz model for insulators) or “free” (Drude model for metals). In other words, electrons are *localized* in insulators and *delocalized* in metals. Switching to quantum physics, this clearcut distinction is apparently lost. The insulating/metallic behavior is typically explained by means of band structure theory, focussing on the position of the Fermi level of the given material: either in a band gap (insulators), or across a band (metals). This explanation addresses the spectrum of the system, hence the nature of the low lying electronic *excitations*. Instead, at a more fundamental level, the qualitative difference in the dc conductivity at low temperature must reflect a qualitative difference in the organization of the electrons in their *ground state*. Such a difference is far from evident in a band-structure picture: the occupied states are of the Bloch form both in insulators and in metals, and qualitatively rather similar (in particular those of simple metals and of simple semiconductors).

In a milestone paper published in 1964, W. Kohn was able to define the insulating state of matter in a way which is reminiscent of the classical picture: he gave evidence that even in a many-electron wavefunction the main feature determining the insulating behaviour is electron localization.³ Although this work mainly addressed *correlated* many-electron systems, its message is very relevant even for materials where an independent-electron approach is quite adequate, as the semiconductor crystals studied here. Much later (1999), Kohn’s outstanding message was analyzed in the light of the modern theory of polarization:^{4–8} a different approach to electron localization was proposed by Resta and Sorella,⁹ hereafter cited as RS. Their starting point is an alternative phenomenological characterization of the insulating/metallic behavior: no direct reference to the dc conductivity is made, while in its

stead macroscopic dielectric polarization is addressed.

Suppose we expose a finite macroscopic sample to an electric field, say inserting it in a charged capacitor. Then the induced macroscopic polarization is qualitatively different in metals and insulators. In the former materials polarization is trivial: universal, material-independent, due to surface phenomena only (screening by free carriers). Therefore polarization in metals is *not* a bulk phenomenon. The opposite is true for insulators: macroscopic polarization is a nontrivial, material-dependent, bulk phenomenon. We can therefore phenomenologically characterize an insulator, in very general terms, as a material whose ground wavefunction sustains a nonzero bulk macroscopic polarization whenever the electronic Hamiltonian is non centrosymmetric. If the Hamiltonian is instead centrosymmetric, the polarization vanishes but remains a well defined bulk property, at variance with the metallic case. There have been sweeping advances in the theory of dielectric polarization since 1992 onwards: the modern theory, where macroscopic polarization is regarded as a Berry phase of the electronic wavefunction,^{4–8} revolutionizes both the very definition of the relevant bulk observable, and the ways to compute it in real solids.

The phenomenological link between macroscopic polarization and insulating behavior was first pointed out and exploited to address electron localization by RS in 1999: even this paper, like Kohn’s 1964 one, mostly concerns correlated systems. Furthermore, in order to keep the presentation simple and concise, most results are explicitly shown in one dimension, while the d -dimensional formulation is only sketched in the final paragraphs of RS. In the present paper we provide a full account of the RS theory of localization in three dimensions, specializing to a sistem of noninteracting electrons, like the band insulators chosen as case studies here.

Two other important papers must be mentioned at this point. In 1997 Marzari and Vanderbilt,¹⁰ hereafter cited as MV, while not addressing metals at all (and hence their difference from insulators), establish nonetheless some results which are relevant to the present viewpoint. In a very recent comprehensive paper¹¹ Souza, Wilkens, and Martin—hereafter cited as SWM—generalize and extend in various ways the main finding of RS:

among other things, they introduce a “cumulant generating function”, whose implications for the present work we discuss.

The paper is organized as follows. In Sect. II we define the basic ingredients providing both polarization and localization, namely the expectation values of the many-body phase operators $z_N^{(\alpha)}$ for the three Cartesian coordinates, Eq. (4). These quantities are vanishing in metals and nonvanishing in insulators, thus qualitatively discriminating between an insulating and a metallic *ground state*. In Sect. III we show, following Ref. 8, how the phase of $z_N^{(\alpha)}$ yields the macroscopic polarization of an insulating crystal: we thus reformulate in a very compact way the modern theory of polarization.^{4,5} In Sect. IV, following RS, we show how the modulus of $z_N^{(\alpha)}$ can be used to define a very meaningful quantity, the localization tensor, for which we adopt the SWM notations: such tensor is finite in insulators and diverges in metals. In Sect. V we discuss the main properties of the localization tensor, and in Sect. VI we present first-principle calculations for several elemental and binary semiconductors: the main trends are analyzed. In Sect. VII we calculate orbitals which are optimally localized in a given direction, and whose average quadratic spread coincides with the localization tensor. We also heuristically check the exponential localization of these orbitals, which we call “hermaphrodite orbitals”. In Sect. VIII we draw our main conclusions. In Appendix A we adapt to our purposes the cumulant generating function of SWM and we show its relevance to the present work. In Appendix B we consider a molecule or a cluster and we discuss our localization tensor therein, showing its relationship to some results of Boys localization theory,¹² well known in quantum chemistry.¹³

II. MANY-BODY PHASE OPERATORS: INSULATORS AND METALS

We are addressing here, as it is done by MV, a crystalline system of independent-electrons, having in mind a Kohn-Sham scheme. The properties of interest, namely, macroscopic polarization and electron localization, are not properties of the individual KS orbitals: instead, they are global properties of the occupied KS manifold. As shown in

Refs. 8,9, it proves formally convenient to deal with a many-body wavefunction Ψ , obtained as a Slater determinant of occupied orbitals. This determinant is uniquely determined by the manifold of the occupied orbitals and is invariant by unitary transformation of these orbitals among themselves: for instance, in insulating crystals, an important transformation of this class converts the occupied Bloch orbitals into Wannier functions.¹⁴ Quantities which can be expressed solely in terms of Ψ are invariant in form under such transformations.

Throughout this work—with the exception of Appendix B—we adopt periodic Born–von–Kàrmàn boundary conditions (BvK) on a large cell, multiple of the crystalline elementary cell. The quantities of interest are intensive and have a well defined thermodynamic limit, while the wavefunction itself becomes an ill-defined mathematical object in that limit.

For the sake of simplicity, we assume a simple cubic cell of side a and a large BvK cell of side $L = Ma$. More general structures can be dealt with using scaling, similarly to what shown *e.g.* in Ref. 5 or in SWM. The thermodynamic limit corresponds to $M \rightarrow \infty$, while practical calculations are performed at finite, and possibly large, M values. The spinorbitals $\psi_{n\mathbf{q}}$ (spin-up) and $\bar{\psi}_{n\mathbf{q}_s}$ (spin-down) may be chosen of the Bloch form. In the finite system there are M^3 allowed Bloch vectors \mathbf{q}_s , arranged on a regular mesh in the unit reciprocal cell, where $s \equiv (s_1, s_2, s_3)$ and

$$\mathbf{q}_s = \frac{2\pi}{Ma}(s_1, s_2, s_3), \quad s_\alpha = 0, 1, \dots, M-1. \quad (1)$$

We adopt a plane-wave-like normalization for the Bloch orbitals:

$$\langle \psi_{n\mathbf{q}_s} | \psi_{n'\mathbf{q}_{s'}} \rangle = \frac{1}{L^3} \int_{\text{BvK cell}} d\mathbf{r} \psi_{n\mathbf{q}_s}^*(\mathbf{r}) \psi_{n'\mathbf{q}_{s'}}(\mathbf{r}) = \delta_{nn'} \delta_{ss'}, \quad (2)$$

If the system is insulating with n_b doubly occupied bands, there are $N = 2n_b M^3$ independent spinorbitals, out of which we write a single-determinant many-body wavefunction for N electrons:

$$\Psi = \mathbf{A} \prod_{n,s} \frac{1}{L^3} \psi_{n\mathbf{q}_s} \bar{\psi}_{n\mathbf{q}_s}, \quad (3)$$

where the product runs over all occupied bands and all mesh points, \mathbf{A} is the antisymmetrizer operator, and the factor ensures that the N -body wavefunction is normalized to one on the

hypercube of side L . If, instead, the system is metallic, then the many-body wavefunction Ψ can still be written in the form of Eq. (3), but where not all the Bloch vectors of a given band are included in the product. We anticipate that this *qualitative* difference has outstanding implications in the following of this work.

According to Refs. 8,9, the key quantities to deal with both macroscopic polarization and electron localization are expectation values of “many-body phase operators”. For a three-dimensional system there are three such operators, one for each Cartesian direction. We indicate as $z_N^{(\alpha)}$, where α is a Cartesian index, their ground-state expectation values:

$$z_N^{(x)} = \langle \Psi | e^{i \frac{2\pi}{L} \sum_{i=1}^N x_i} | \Psi \rangle, \quad (4)$$

and analogously for y and z directions. This remarkably compact expression is very general and applies as it stands even to correlated and/or disordered systems: here we specialize to a crystalline system of independent electrons, whose wavefunction Ψ assumes the form of Eq. (3), where the product indices have to be differently specified in the insulating and metallic cases. The many-body expectation values $z_N^{(\alpha)}$ contain, in the large N limit, all the information about macroscopic polarization and—in cubic or high-symmetry materials—about electron localization as well. The case of low-symmetry materials is discussed in Appendix A.

We may conveniently recast $z_N^{(x)}$ as an overlap

$$z_N^{(x)} = \langle \Psi | \tilde{\Psi} \rangle, \quad (5)$$

where $\tilde{\Psi}$ is the Slater determinant of a different set of Bloch spinorbitals:

$$\tilde{\psi}_{n\mathbf{q}_s}(\mathbf{r}) = e^{i \frac{2\pi}{Ma} x} \psi_{n\mathbf{q}_s}(\mathbf{r}), \quad (6)$$

and analogously for the bar (spin-down) ones. According to a well known theorem, the overlap between two single-determinant wavefunctions is equal to the determinant of the $N \times N$ overlap matrix built out of the occupied spinorbitals. Since the overlaps between different-spin spinorbitals vanish, and those between equal-spin ones are identical in pairs, we can write

$$z_N^{(x)} = (\det \mathcal{S})^2, \quad (7)$$

where \mathcal{S} is the overlap matrix between spatial orbitals, having size $N/2 = n_b M^3$. Its elements are:

$$\begin{aligned} \mathcal{S}_{n\mathbf{q}_s, n'\mathbf{q}_{s'}} &= \frac{1}{L^3} \int_{\text{BvK cell}} d\mathbf{r} \psi_{n\mathbf{q}_s}^*(\mathbf{r}) \tilde{\psi}_{n'\mathbf{q}_{s'}}(\mathbf{r}) \\ &= \frac{1}{L^3} \int_{\text{BvK cell}} d\mathbf{r} u_{n\mathbf{q}_s}^*(\mathbf{r}) u_{n'\mathbf{q}_{s'}}(\mathbf{r}) e^{i(\frac{2\pi}{Ma}x + \mathbf{q}_{s'} \cdot \mathbf{r} - \mathbf{q}_s \cdot \mathbf{r})}, \end{aligned} \quad (8)$$

where the u 's are the periodic functions in the Bloch orbitals.

The matrix \mathcal{S} is very sparse: in fact, given the geometry of the \mathbf{q}_s 's on the regular reciprocal mesh (see Eq. (1), the overlap integrals in Eq. (8) are nonvanishing only if $s_1 = s'_1 + 1$, $s_2 = s'_2$, and $s_3 = s'_3$. We express the nonvanishing elements in terms of a small overlap matrix S , of size $n_b \times n_b$:

$$S_{nn'}(\mathbf{q}, \mathbf{q}') = \langle u_{n\mathbf{q}} | u_{n'\mathbf{q}'} \rangle = \frac{1}{a^3} \int_{\text{cell}} d\mathbf{r} u_{n\mathbf{q}}^*(\mathbf{r}) u_{n'\mathbf{q}'}(\mathbf{r}). \quad (9)$$

Owing to the sparseness of \mathcal{S} , its determinant factors into products of determinants of small matrices S .

In the insulating case we use the wavefunction of Eq. (3), where all the Bloch vectors of a given band are occupied: the factorization is then

$$z_N^{(x)1/2} = \det \mathcal{S} = \prod_s \det S(\mathbf{q}_{s_1+1, s_2, s_3}, \mathbf{q}_{s_1, s_2, s_3}). \quad (10)$$

We get a more compact notation upon defining

$$\Delta \mathbf{q}^{(x)} = \frac{2\pi}{L}(1, 0, 0) = \frac{2\pi}{Ma}(1, 0, 0), \quad (11)$$

which is the vector connecting nearest neighbor \mathbf{q} points in the x direction. We have then:

$$z_N^{(x)1/2} = \prod_s \det S(\mathbf{q}_s + \Delta \mathbf{q}^{(x)}, \mathbf{q}_s); \quad (12)$$

In the metallic case, instead, the $z_N^{(\alpha)}$'s are identically zero. This is easily understood by looking at the simple case with only one band. Suppressing the band index the small overlap

matrix becomes a c-number $S(\mathbf{q}, \mathbf{q}')$, and Eq. (10) becomes a product of c-numbers, with no determinant to evaluate. In an insulator this product runs over the whole \mathbf{q}_s mesh, and all factors are nonzero; in a metal the analogous product runs only on the \mathbf{q}_s 's within the Fermi surface. Looking at the definition of $S(\mathbf{q}, \mathbf{q}')$, Eqs. (8) and (9), it is clear that there exists at least one occupied \mathbf{q}_s , adjacent to the Fermi surface, such that $S(\mathbf{q}_s, \mathbf{q}_{s'})$ vanishes for all *occupied* s' . This is enough to imply that $z_N^{(\alpha)}$ vanishes as well.

We have thus arrived at one of the important results of this paper. The complex numbers $z_N^{(\alpha)}$ are ground-state expectation values, and do not access any spectral information. Yet they qualitatively discriminate between insulators and metals: they are in fact nonvanishing in the former materials, and vanishing in the latter ones. In agreement with Kohn's viewpoint,³ we are showing in a novel way that there is indeed a qualitative difference in the organization of the electrons in their ground state. It is remarkable that, in the present case, such difference shows up already at *finite* N , before the thermodynamic limit is taken.

III. MACROSCOPIC POLARIZATION

In centrosymmetric materials the expectation values $z_N^{(\alpha)}$ are real (provided the origin is chosen at a centrosymmetric site), while in noncentrosymmetric materials they are in general complex: their phases define then the Cartesian components of the macroscopic polarization in suitable units. In the metallic case the $z_N^{(\alpha)}$'s vanish and the polarization is ill defined, in agreement with the phenomenological viewpoint illustrated in Sect. I. We anticipate that, as first proposed by RS, the moduli of $z_N^{(\alpha)}$ will be used to provide a quantitative measure of electron localization in insulators.

When discussing macroscopic polarization, it should be kept in mind that the “absolute” polarization of a given sample has never been measured as a bulk property: one invariably measures derivatives (dielectric constants, piezoelectric coefficients, dynamical charges....) or finite differences (polarization reversal in ferroelectrics).^{5,7} Furthermore, the quantity actually measured is the current \mathbf{J} which traverses the sample while the given perturbation

is adiabatically switched on. One is therefore interested into the quantity

$$\Delta \mathbf{P} = \int_0^{\Delta t} dt \langle \mathbf{J}(t) \rangle : \quad (13)$$

in the adiabatic limit Δt goes to infinity and $\mathbf{J}(t)$ goes to zero, while $\Delta \mathbf{P}$ depends on the initial and final states.

It has been shown in Ref. 8 that the electronic contribution to $\Delta \mathbf{P}$ can be expressed as a “two-point formula” in terms of the phases (Berry phases¹⁵) of the $z_N^{(\alpha)}$ ’s. We neglect the ionic contribution from now on, and we write:

$$\Delta P_\alpha = \frac{e}{2\pi L^2} [\text{Im} \ln z_N^{(\alpha)}(\Delta t) - \text{Im} \ln z_N^{(\alpha)}(0)], \quad (14)$$

where e is the electron charge ($e < 0$ here, as well as in many other papers, including Ref. 5). The thermodynamic limit $M \rightarrow \infty$, hence $L \rightarrow \infty$ and $N \rightarrow \infty$, is implicitly understood. The proof of Eq. (14) provided in Ref. 8 is quite general and valid even for correlated and/or disordered many-body wavefunctions: however in order to keep the presentation simple and concise, most results are explicitly shown in one dimension, while the three-dimensional formulation is only sketched in the final paragraphs of Ref. 8. Here we provide the complete three-dimensional formulation in the independent-electron case, and we show how the thermodynamic limit of Eq. (14) yields the—by now famous—Berry phase formula for the macroscopic polarization of a crystalline system of independent electrons, first discovered by King-Smith and Vanderbilt in 1993.^{4,5,7}

From Eq. (12) we get

$$\ln z_N^{(x)} = -2 \sum_{s_2, s_3=0}^{M-1} \ln \prod_{s_1=0}^{M-1} \det S(\mathbf{q}_s, \mathbf{q}_s + \Delta \mathbf{q}^{(x)}), \quad (15)$$

which replaced into Eq. (14) yields

$$P_x = -\frac{e}{\pi M^2 a^2} \sum_{s_2, s_3=0}^{M-1} \text{Im} \ln \prod_{s_1=0}^{M-1} \det S(\mathbf{q}_s, \mathbf{q}_s + \Delta \mathbf{q}^{(x)}). \quad (16)$$

As already observed, crystal lattices different from the simple cubic one can be easily dealt with by scaling, as shown in detail in Ref. 5 or in SWM. It is understood that Eq. (16)

has to be used twice, with the final and with the initial ground states, in order to evaluate the quantity of interest $\Delta\mathbf{P}$. Eq. (16) is very similar, but not yet identical, to the formula actually implemented in practical calculations,^{4,5} where the crucial difference concerns the “polarization quantum”. Since in Eq. (16) each term in the sum is arbitrary modulo 2π , P_α is determined only modulo $\frac{2e}{M^2a^2}$, which becomes vanishingly small in the thermodynamic limit. Instead we know, from the modern theory of polarization,^{4,5} that the genuine “quantum” is M –independent: P_α is determined modulo $\frac{2e}{a^2}$. One must then proceed as follows: let us define

$$\gamma_{s_2,s_3} = -\text{Im} \ln \prod_{s_1=0}^{M-1} \det S(\mathbf{q}_s, \mathbf{q}_s + \Delta\mathbf{q}^{(x)}); \quad (17)$$

$$P_x = \frac{e}{\pi a^2} \frac{1}{M^2} \sum_{s_2,s_3=0}^{M-1} \gamma_{s_2,s_3}. \quad (18)$$

The quantity γ_{s_2,s_3} can be regarded as the discretization over a mesh of a dimensionless function $\gamma(q_y, q_z)$ defined in the two–dimensional unit reciprocal cell $[0, 2\pi/a) \times [0, 2\pi/a)$. For a dense mesh one obviously gets

$$\sum_{s_2,s_3} \gamma_{s_2,s_3} \rightarrow \frac{L^2}{(2\pi)^2} \int dq_y dq_z \gamma(q_y, q_z), \quad (19)$$

and Eq. (18) becomes in the thermodynamic limit

$$P_x = \frac{2e}{(2\pi)^3} \int dq_y dq_z \gamma(q_y, q_z). \quad (20)$$

We pause at this point to emphasize two issues, made very clear by the present derivation. First: the role played by the polarization quantum. The phase $\gamma(q_y, q_z)$ is arbitrary modulo 2π , but we tacitly assume it to be a *continuous function* in its domain. Therefore any choice of the “quantum” at a given (q_y, q_z) fixes the arbitrariness throughout the whole domain $[0, 2\pi/a) \times [0, 2\pi/a)$: this is the reason why the quantum incertitude in Eq. (20) assumes now the desired value of $\frac{2e}{a^2}$. Second: the role played by crystalline periodicity. If we describe a disordered system using a fictitious periodicity over a large “supercell” (large a), then the

“quantum” in three dimensions is indeed small, and only small polarization differences $\Delta\mathbf{P}$ can be unambiguously evaluated by means of the two-point formula, Eq. (14).

The quantities in Eq. (17) are precisely those evaluated in actual calculations, where the crystal Hamiltonian is diagonalized over a discrete mesh in reciprocal space. In order to recover the continuum formulation of Refs. 4,5 we need to perform the $M \rightarrow \infty$ limit. Supposing $u_{n\mathbf{q}}$ are differentiable functions of \mathbf{q} , the limit reads:

$$\begin{aligned} & - \lim_{M \rightarrow \infty} \text{Im} \ln \prod_{s_1=0}^{M-1} \det S(\mathbf{q}_s, \mathbf{q}_s + \Delta\mathbf{q}^{(x)}) \\ & = i \sum_{n=1}^{n_b} \int_{C_{s_2, s_3}} dq_x \langle u_{n\mathbf{q}} | \frac{\partial}{\partial q_x} u_{n\mathbf{q}} \rangle, \end{aligned} \quad (21)$$

where C_{s_2, s_3} is the straight-line segment which joins the reciprocal points $(0, q_{s_2}, q_{s_3})$ and $(2\pi/a, q_{s_2}, q_{s_3})$, differing by a reciprocal lattice vector. The proof of Eq. (21) has been reported several times;^{5,15} an alternate proof is given in Appendix A.

Putting the above results together we arrive at the thermodynamic limit in the form of:

$$P_x = \frac{2ie}{(2\pi)^3} \sum_{n=1}^{n_b} \int d\mathbf{q} \langle u_{n\mathbf{q}} | \frac{\partial}{\partial q_x} u_{n\mathbf{q}} \rangle, \quad (22)$$

where the integral is performed over the reciprocal unit cell, or equivalently over the first Brillouin zone. Eq. (22) is precisely the well known King-Smith and Vanderbilt expression of the (continuum) Berry-phase theory of polarization.^{4,5}

IV. ELECTRON LOCALIZATION

In Sect. II we have defined the three expectation values of the many-body phase operators, Eq. (4) and analogues, and we have shown that they provide the macroscopic polarization of the crystalline sample. Here we address electron localization using essentially the moduli of these same $z_N^{(\alpha)}$'s. Following RS, electron localization is measured by a squared localization length in one dimension, and by a “localization tensor” in three dimensions. This tensor is an intensive quantity, has the dimensions of a squared length, and measures the localization of the many-electron system as a whole: in the present case, it is a global

property of the occupied KS manifold. The localization tensor is finite for insulators and diverges for metals.

In the very recent SWM paper¹¹ it is shown, among other things, that the RS localization tensor is related to the mean-square quantum fluctuation of the polarization: it is a second cumulant moment, which can be very elegantly extracted from a moment generating function. In Appendix A we show the way how the SWM approach works in the present case. We adopt throughout notations inspired by SWM, and we indicate the localization tensor as $\langle r_\alpha r_\beta \rangle_c$, where the subscript stays for “cumulant”. For a material having cubic or tetrahedral symmetry, like the semiconductors considered in the present case studies, the localization tensor is isotropic: its only independent element is $\langle x^2 \rangle_c$. Its expression is provided by RS, whose Eq. (18) we recast here as

$$\langle x^2 \rangle_c = -\frac{1}{N} \left(\frac{L}{2\pi} \right)^2 \ln |z_N^{(x)}|^2, \quad (23)$$

and the thermodynamic limit is understood. For a metal $z_N^{(x)}$ vanishes and the localization tensor is formally infinite, even at finite N . For an insulator, whose wavefunction has the form of Eq. (3), we get from Eq. (12)

$$|z_N^{(x)}| = \prod_s \det S^\dagger(\mathbf{q}_s, \mathbf{q}_s + \Delta\mathbf{q}^{(x)}) S(\mathbf{q}_s, \mathbf{q}_s + \Delta\mathbf{q}^{(x)}); \quad (24)$$

$$\langle x^2 \rangle_c = -\left(\frac{a}{2\pi} \right)^2 \frac{1}{2n_b M} \ln |z_N^{(x)}|^2. \quad (25)$$

Eqs. (24) and (25) are the typical expressions implemented in our test-case calculations discussed below. The thermodynamic limit is obtained as usual for $M \rightarrow \infty$ and takes, not surprisingly, the form of an integral performed over the reciprocal unit cell, or equivalently over the first Brillouin zone. The integral is:

$$\begin{aligned} \langle x^2 \rangle_c = \frac{a^3}{n_b (2\pi)^3} \int d\mathbf{q} \left(\sum_n \left\langle \frac{\partial}{\partial q_x} u_{n\mathbf{q}} \middle| \frac{\partial}{\partial q_x} u_{n\mathbf{q}} \right\rangle \right. \\ \left. - \sum_{n,n'} \left\langle u_{n\mathbf{q}} \middle| \frac{\partial}{\partial q_x} u_{n'\mathbf{q}} \right\rangle \left\langle \frac{\partial}{\partial q_x} u_{n'\mathbf{q}} \middle| u_{n\mathbf{q}} \right\rangle \right). \end{aligned} \quad (26)$$

The proof is relatively straightforward, starting from Eq. (26) and discretizing integrals and derivatives on the mesh defined in Eq. (1). We will provide a more elegant proof, inspired by SWM, in Appendix A.

Expressions such as Eq. (26) and similar ones had appeared in the literature before,¹⁴ in relationship to Wannier functions. By means of an expression of this kind, MV define a ground-state quantity Ω_I which sets a lower bound for the second (spherical) moments of the Wannier functions.¹⁰ More precisely, for an insulator with n_b occupied bands (hence n_b Wannier functions per cell) such second moment is no smaller in average than Ω_I/n_b . It is worth mentioning at this point that the logic of the MV paper goes backwards with respect to the present approach: first they provide a continuum theory, and then they discretize for computational purposes. Their discretization is different from Eq. (25), which emerges naturally from the present formulation starting from the remarkably compact Eq. (23). Both discretizations obviously converge to the same $M \rightarrow \infty$ limit: their convergence properties are different, though.

Specializing MV to a cubic material, RS have found the simple relationship $\Omega_I = 3n_b\langle x^2 \rangle_c$: notice that $\langle x^2 \rangle_c$ is intensive, while Ω_I is not such. Building upon MV's work, we are now ready to generalize the localization tensor to materials of arbitrary symmetry:

$$\begin{aligned} \langle r_\alpha r_\beta \rangle_c = & \frac{V_c}{n_b(2\pi)^3} \int d\mathbf{q} \left(\sum_n \left\langle \frac{\partial}{\partial q_\alpha} u_{n\mathbf{q}} \middle| \frac{\partial}{\partial q_\beta} u_{n\mathbf{q}} \right\rangle \right. \\ & \left. - \sum_{n,n'} \left\langle u_{n\mathbf{q}} \middle| \frac{\partial}{\partial q_\alpha} u_{n'\mathbf{q}} \right\rangle \left\langle \frac{\partial}{\partial q_\beta} u_{n'\mathbf{q}} \middle| u_{n\mathbf{q}} \right\rangle \right), \end{aligned} \quad (27)$$

where V_c is the cell volume. Notice that the imaginary part of the integrand in Eq. (27), being antisymmetric in \mathbf{q} , cancels in the integral, such that the localization tensor is real. Even the offdiagonal elements, as defined in Eq. (27), have a finite- N counterpart, which is discussed in Appendix A.

For an insulating crystal of arbitrary symmetry, Ω_I as defined by MV equals n_b times the trace of our localization tensor $\langle r_\alpha r_\beta \rangle_c$. In a metal, expressions like Eqs. (26) and (27) do not make much sense, consistently with the fact that our finite- N expression, Eq. (23),

is formally infinite at any N value.

V. PROPERTIES OF THE LOCALIZATION TENSOR

We have already emphasized that the localization tensor is a property of the occupied KS manifold as a whole. The main quantity which defines such manifold is the (spin-integrated) single-particle density matrix ρ , which coincides with twice the projector P over the occupied KS orbitals: this projector is invariant by unitary transformations of the orbitals. using Bloch eigenfunctions the projector reads, for an insulator with n_b occupied bands:

$$P(\mathbf{r}, \mathbf{r}') = \frac{1}{2}\rho(\mathbf{r}, \mathbf{r}') = \frac{1}{(2\pi)^3} \sum_{n=1}^{n_b} \int d\mathbf{q} \psi_{n\mathbf{q}}(\mathbf{r}) \psi_{n\mathbf{q}}^*(\mathbf{r}'). \quad (28)$$

The localization tensor (in the thermodynamic limit) has been written as a Brillouin-zone integral in Eq. (27). This integral can be identically transformed into a particularly simple expression whose only ingredient is P :

$$\langle r_\alpha r_\beta \rangle_c = \frac{1}{2n_b} \int_{\text{cell}} d\mathbf{r} \int_{\text{all space}} d\mathbf{r}' (\mathbf{r} - \mathbf{r}')_\alpha (\mathbf{r} - \mathbf{r}')_\beta |P(\mathbf{r}, \mathbf{r}')|^2, \quad (29)$$

which is the second moment of the (squared) density matrix in the coordinate $\mathbf{r} - \mathbf{r}'$. The proof of the equivalence between Eq. (29) and Eq. (27) can be worked out using the same algebra appearing in Ref. 14: for a different argument proving the same result, see Appendix B.

We have arrived at Eq. (29) considering an insulating crystal so far. In this case we know, under general arguments,^{16–19} that $P(\mathbf{r}, \mathbf{r}')$ is asymptotically exponential in the argument $|\mathbf{r} - \mathbf{r}'|$: this confirms that the integral over all space in Eq. (29) converges and the localization tensor is therefore finite. At this point, it is worthwhile to apply the general form of Eq. (29) to the metallic case. For the simplest metal of all, the free electron gas, the density matrix is known exactly:²⁰

$$P(\mathbf{r}, \mathbf{r}') = \frac{1}{2}\rho(\mathbf{r}, \mathbf{r}') = \frac{3n_0}{2} \frac{j_1(k_F |\mathbf{r} - \mathbf{r}'|)}{k_F |\mathbf{r} - \mathbf{r}'|}. \quad (30)$$

Replacement of Eq. (30) into Eq. (29) results in a diverging integral, thus confirming that our localization tensor is formally infinite in this paradigmatic metal. Other, more realistic, metals feature this same divergence.

The fact that the density matrix $\rho(\mathbf{r}, \mathbf{r}')$ is short-range in the variable $\mathbf{r} - \mathbf{r}'$ has been named “nearsightedness” by W. Kohn.¹⁸ The second moment expression in Eq. (29) shows that our localization tensor is indeed a meaningful quantitative measure of such nearsightedness. We are going to analyze below the major trends over an important class of materials: tetrahedral semiconductors. We mention at this point that a conceptually different measure of the nearsightedness of a given electronic ground state focusses instead on the exponent governing the exponential decay of $\rho(\mathbf{r}, \mathbf{r}')$ in insulators: some case studies have been recently investigated.^{19,21}

We have already observed that some of our findings are closely related to the previous work by MV. These authors’ main interest were the “optimally localized Wannier functions”, *i.e.* those localized orbitals which minimize the average spherical moment. They prove, among other things, that such moment is strictly larger than the trace of our localization tensor. Building on their results, it is straightforward to attribute a similar meaning to the tensor itself: for any transformation of the occupied orbitals into a set of unitarily equivalent ones, the second moment in a given direction can be no smaller than the localization tensor, projected on that direction.

Since we are going to apply our results to cubic materials only, we focus on those orbitals which minimize in average the quadratic spread (second moment) in the x coordinate. These orbitals turn out to be localized (Wannier-like) in the x direction and completely delocalized (Bloch-like) in the orthogonal direction: they therefore deserve the name of “hermaphrodite orbitals”. The present formalism makes the definition of these orbitals particularly simple: they are in fact the eigenfunctions of the position operator x , projected over the occupied manifold. Calling $\Xi = PxP$ this operator, its expression in the Schrödinger representation is:

$$\Xi(\mathbf{r}, \mathbf{r}') = \int_{\text{all space}} d\mathbf{r}'' P(\mathbf{r}, \mathbf{r}'') x'' P(\mathbf{r}'', \mathbf{r}'). \quad (31)$$

Notice that x is *incompatible* with BvK boundary conditions and its matrix elements over Bloch states are ill defined; nonetheless, Ξ is—in insulators—a well defined operator, which maps any vector of the occupied manifold into another vector of the same manifold. This fact owes to the exponential localization of P in Eq. (31).

The relationship between Ξ and the hermaphrodite orbitals optimally localized in the x direction is easily proved borrowing some results from MV; for a different argument leading to the same proof, see Appendix B. We also notice an important difference with respect to the three-dimensional localization explicitly considered by MV. While the trace of the localization tensor provides a *lower bound* for three-dimensional localization, its element $\langle x^2 \rangle_c$ provides instead a genuine *minimum* for one-dimensional localization (in a cubic material). This qualitative difference owes to the fact that, while one can manifestly diagonalize PxP , one cannot simultaneously diagonalize PxP , PyP , and PzP .

We end this Section about the properties of the localization tensor with a most important issue: is $\langle r_\alpha r_\beta \rangle_c$ a measurable quantity? The answer, due to SWM, is “yes”. They prove the identity:

$$\langle r_\alpha r_\beta \rangle_c = \frac{\hbar V_c}{2\pi e^2 n_b} \int_0^\infty \frac{d\omega}{\omega} \text{Re } \sigma_{\alpha\beta}(\omega), \quad (32)$$

where $\sigma_{\alpha\beta}$ is the conductivity tensor. Notice that the left hand side, as emphasized throughout the present work, is a property of the electronic *ground state*, while the right hand side is a measurable property related to electronic *excitations*: therefore Eq. (32) must be regarded as a sum rule. The frequency integral in Eq. (32) diverges in metals and is finite in insulators, as obviously expected. Since in the latter materials there is a gap for electronic excitations, Eq. (32) immediately leads to the inequality:

$$\langle r_\alpha r_\beta \rangle_c < \frac{\hbar V_c}{2\pi e^2 n_b \varepsilon_g} \int_0^\infty d\omega \text{Re } \sigma_{\alpha\beta}(\omega), \quad (33)$$

where ε_g is the direct gap. Using then the oscillator–strength sum rule, Eq. (33) for a cubic material is cast as:

$$\langle x^2 \rangle_c < \frac{\hbar^2}{2m_e \varepsilon_g}. \quad (34)$$

Below, we investigate the trends in both members of this inequality for our test-case materials.

VI. CALCULATED LOCALIZATION TENSORS

We have studied several tetrahedrally coordinated crystalline materials, from the group IV, III–V, and II–VI, having the diamond and zincblende structure. The first-principle calculations have been performed within density-functional theory in the local-density approximation, using pseudopotentials²² and plane waves. We implement a trivial extension of the formulas presented above, using a rectangular unit cell instead of a simple cubic one: we thus describe the diamond and zincblende structures by means of a tetragonal cell with a lattice constant a in the basal plane and $c = \sqrt{2}a$. There are four atoms per unit cell, whose projections on the c axis are equispaced; for the sake of consistency with the formal results, we take x along the c axis and yz in the basal plane. We then use a BvK cell of sides $M_x c$, $M_y a$, and $M_z a$, corresponding to a mesh in reciprocal space with M_x, M_y, M_z points: this allows an easier control of convergence.

We start evaluating at the mesh points the Hermitian matrices

$$A_s = S^\dagger(\mathbf{q}_s, \mathbf{q}_s + \Delta\mathbf{q}^{(x)}) S(\mathbf{q}_s, \mathbf{q}_s + \Delta\mathbf{q}^{(x)}); \quad (35)$$

then Eqs. (24) and (25) are written as

$$\langle x^2 \rangle_c = \frac{1}{M_y M_z} \sum_{s_2=1}^{M_y} \sum_{s_3=1}^{M_z} \left(-\frac{c^2 M_x}{4\pi^2 n_b} \sum_{s_1=1}^{M_x} \ln \det A_s \right). \quad (36)$$

In general convergence is fast in M_y , M_z , and slower in M_x . The expression in parenthesis in Eq. (36) is precisely the one-dimensional expression discussed in detail by RS, and the three dimensional one simply obtains from it as an average in the (q_y, q_z) plane.

First we show in Fig. 1 the convergence of our expressions over a genuinely cubic grid, which coincides with the one used by MV in their evaluation of the quantity $\Omega_I = 3n_b \langle x^2 \rangle_c$.

They use a different discretization of the same \mathbf{k} space integral: both calculations converge to the same localization tensor, although our discretization, based on Eqs. (24) and (25), converges faster. All the following results have been obtained using noncubic grids, as in Eq. (36), in order to achieve faster convergence.

We have systematically calculated well converged localization tensors for several elemental and binary semiconductors. In Fig. 2 we plot the localization tensors versus the right-hand member of the inequality in Eq. (34), where for the gap ε_g we have used both the theoretical and the experimental values. The use of the former is a check of the internal consistency of the theoretical results; the use of the latter is motivated by the fact that density-functional theory in the local-density approximation provides a good representation of the ground state, but not of the excited ones. In both ways, the inequality is very strongly verified for all materials. The localization tensor ranges roughly between 1 and 3 bohr² for all the material considered, diamond being the most localized and germanium the most delocalized. The trend is qualitatively expected, in agreement with SWM’s statement that “the larger the gap, the more localized the electrons are”: however a few materials violate this trend (compare *e.g.* AlAs with ZnSe). Regularities can be observed when comparing families of materials: either isoelectronic series or isovalent series. In order to enhance such regularities, we have heuristically tried a few different laws. In Fig. 3 we plot our localization tensor versus $1/\varepsilon_g$, using the minimum gaps instead of the direct ones: here monotonical trends are very perspicuous.

VII. HERMAPHRODITE ORBITALS

We actually perform here localizing trasformations on the (delocalized) Bloch orbitals. At variance with the work of MV, we focus on orbitals which are optimally localized in one direction only, say x , while they are completely delocalized in the yz directions: this is the reason for naming them “hermaphrodite orbitals”. It has been shown that, in the thermodynamic limit, these orbitals are eigenfunctions of the operator Ξ , Eq. (31), and their

centers are the corresponding eigenvalues. It is expedient to consider the modified operator

$$\tilde{\Xi}(\mathbf{r}, \mathbf{r}') = \int_{\text{all space}} d\mathbf{r}'' P(\mathbf{r}, \mathbf{r}'') e^{i\frac{2\pi}{M_x c} x''} P(\mathbf{r}'', \mathbf{r}'), \quad (37)$$

which to leading order in $1/M_x$ has the same eigenfunctions as Ξ , and simply related eigenvalues.

When considering a finite sample with BvK boundary conditions—or equivalently a discrete grid in the reciprocal unit cell—the operator Ξ as in Eq. (31) is useless because the operator x therein becomes ill defined. Instead the operator $\tilde{\Xi}$ is well defined, provided the value of M_x is consistent with the choice of the grid. The integral in Eq. (37) is now performed over the BvK cell and *not* over all space; the projector projects over the finite occupied manifold, having dimension $n_b M_x M_y M_z$. Choosing the Bloch functions as the basis in the occupied manifold, the matrix elements of $\tilde{\Xi}$ are nothing else than the matrix \mathcal{S} defined in Eq. (8). Therefore in the discrete case the hermaphrodite orbitals which achieve optimal localization in the x direction are simply obtained by diagonalizing the matrix \mathcal{S} . Since, as already observed, the matrix is already diagonal in s_2 and s_3 , the problem is reduced to $M_y M_z$ independent diagonalizations of submatrices of size $n_b M_x$. We characterize our orbitals as w_{j,s_2,s_3} , where (s_2, s_3) is a two-dimensional Bloch-index and j is a one-dimensional Wannier-like index, with $1 \leq j \leq n_b M_x$.

We are going to verify that these orbitals indeed minimize the average quadratic spread in one-dimension. If we define

$$z_{j,s_2,s_3} = \int_{\text{BvK cell}} d\mathbf{r} |w_{j,s_2,s_3}(\mathbf{r})|^2 e^{i\frac{2\pi}{M_x c} x}, \quad (38)$$

then according to RS the quadratic spread of one given hermaphrodite orbital is:

$$\langle w_{j,s_2,s_3} | x^2 | w_{j,s_2,s_3} \rangle_c = -\frac{c^2 M_x^2}{4\pi^2} \ln |z_{j,s_2,s_3}|^2. \quad (39)$$

Taking now the average over all orbitals, and calling this quantity λ_{xx}^2 , we get

$$\lambda_{xx}^2 = \frac{1}{M_y M_z} \sum_{s_2=1}^{M_y} \sum_{s_3=1}^{M_z} \left(-\frac{c^2 M_x}{4\pi^2 n_b} \sum_{j=1}^{n_b M_x} \ln |z_{j,s_2,s_3}|^2 \right). \quad (40)$$

We then notice that w_{j,s_2,s_3} are the eigenvectors of $\tilde{\Xi}$, hence the expectation values z_{j,s_2,s_3} are the corresponding eigenvalues. Since the product of the eigenvalues equals the determinant, standard manipulations prove that the average spread λ_{xx}^2 equals indeed the lower bound $\langle x^2 \rangle_c$ as given in Eq. (36).

There is a subtlety about the diagonalization of the submatrices of \mathcal{S} , which are the projection over a certain finite dimensional manifold of the operator $e^{i\frac{2\pi}{M_x c}x}$. Although the operator is unitary, its projection is not a unitary matrix, hence the eigenvectors are not exactly orthogonal, as instead honest localized orbitals must be: this is not a serious problem. In fact the larger is M_x , the closer to unitarity the matrix becomes: we know that the modulus of its determinant differs by one for a term of the order $1/M_x$, hence the modulus of each eigenvalue differs by one for a term of the order $1/M_x^2$. We recover exact orthonormality in the thermodynamic limit; in our calculations already at $M_x \simeq 20$ deviations from orthogonality are hardly noticeable.

We have calculated the orbitals w_{j,s_2,s_3} for several crystalline semiconductors: to the purpose of display, we call the yz average of $|w_{j,s_2,s_3}|^2$ as $n_{\text{loc}}(x)$, where the indices remain implicit. At fixed (s_2, s_3) we have, given our double cell, $8M_x$ orbitals centered on a BvK period of length $M_x c$. There are however at most four different shapes, and one obtains all the functions upon translations in the x direction (by multiples of $c/2$) of the four basic ones: this is not surprising, since the genuine unit cell is one half of our computational one. We find that the different shapes are actually always four, with the only exception of an elemental semiconductor at $s_2 = s_3 = 0$. In this very special case the different shapes are only two, the orbitals are centered at the bond center, and their densities are centrosymmetric: the corresponding functions $n_{\text{loc}}(x)$ are shown in Fig. 4 for the case of Si. The most general case is exemplified by Fig. 5: it shows the four different $n_{\text{loc}}(x)$ for the case of GaAs, again at $s_2 = s_3 = 0$. None of these four w orbitals is therefore centered at a symmetry site, and none is centrosymmetrical, although they are obviously symmetrically related to each other. About the actual value of the quadratic spread (in the x direction) of each of the w 's, we

have found as a general feature that the least localized ones are those for $s_2 = s_3 = 0$, *i.e.* at the Γ point in the two-dimensional reciprocal space.

We now address the long standing issue of exponential localization. For the genuine one-dimensional case W. Kohn has proved long ago¹⁶ that the Wannier functions which minimize the quadratic spread (*i.e.* are optimally localized) have an asymptotic exponential behavior. In three dimensions the problem is unsolved, with the exception of some very special cases. It has been conjectured by MV that their optimally localized Wannier functions enjoy three-dimensional exponential localization: an analytical proof looks very hard. Our hermaphrodite orbitals w are optimally localized in the x direction, and therefore in a sense they have one-dimensional character: nonetheless, they have a genuine dependence on all three coordinates, and an analytic proof along the lines of Kohn’s one-dimensional case looks hard.

Our very elongated BvK cells allow us to study the asymptotic behaviour heuristically on our calculated w ’s. The nearest periodic replica of a given w orbital is centered at a distance of $M_x c$ from it: therefore the interesting “asymptotic region” is accessible up to a distance somewhat smaller than $M_x c/2$, as it clearly appears from Fig. 6. The quantity of choice in order to “blow up” the exponential behavior is obviously the logarithm of $n_{\text{loc}}(x)$, which we plot in Fig. 6 (thin solid lines) for the case of Ge and for two different (s_2, s_3) . It is seen that there is a wide region where the plots have an overall linear behavior, with superimposed oscillations having the crystal periodicity along the x direction ($c/2$ in the present case). The slopes at different (s_2, s_3) are very different, though; the $n_{\text{loc}}(x)$ with the slowest decay corresponds to $s_2 = s_3 = 0$ and therefore to the least localized, as we previously observed. We found that this is also a general feature of the materials studied here. Next, we filter the disturbing periodic oscillations using our favorite tool of the macroscopic average.²³ We tried both ways: filtering $n_{\text{loc}}(x)$ first and then taking the logarithm, or filtering $\ln n_{\text{loc}}(x)$: the latter turns out to work best. The macroscopic filtering is also shown in Fig. 6 (thick solid lines): it is easily realized, especially looking at the magnified plot in the lower panel, that there is a sizeable region, spanning several cells, where the plotted function looks accurately

linear with x , hence $n_{\text{loc}}(x) \propto \exp(\pm bx)$. We therefore demonstrate “experimentally” the exponential localization of our w orbitals. Finally, in Fig. 7 we display some correlations between the localization length and the exponential decay length $1/b$ averaged over the two-dimensional mesh (s_2, s_3) .

VIII. CONCLUSIONS

In the present work we provide the complete three-dimensional formulation of the RS theory of electron localization⁹, specializing it to the case of independent KS electrons; we show how it relates to the MV and SWM papers^{10,11}, and also (in Appendix B) how it relates to Boys theory of localization in molecules¹². We then implement the theory to several materials in the class of tetrahedrally coordinated semiconductors. Among the results, we find that not in all cases the calculated localization length is a monotonical function of the gap, although the trends are regular within a given family (isoelectronic or isovalent). Finally, we heuristically show that the orbitals which are optimally localized in a given direction (“hermaphrodite orbitals”) show exponential localization.

ACKNOWLEDGMENTS

R.R. acknowledges partial support by ONR grant N00014-96-1-0689.

APPENDIX A: CUMULANT GENERATING FUNCTION

We specialize here to our purposes the general concept of generating function introduced very recently¹¹ by SWM. In the present independent-electron scheme this function is defined as

$$\ln C(\mathbf{k}) = \frac{V_c}{n_b(2\pi)^3} \int d\mathbf{q} \ln \det S(\mathbf{q}, \mathbf{q}+\mathbf{k}), \quad (\text{A1})$$

where S is the small overlap matrix of size $n_b \times n_b$ defined in Eq. (9). Using a well known identity, Eq. (A1) can be equivalently written as:

$$\ln C(\mathbf{k}) = \frac{V_c}{n_b(2\pi)^3} \int d\mathbf{q} \operatorname{tr} \ln S(\mathbf{q}, \mathbf{q}+\mathbf{k}). \quad (\text{A2})$$

Supposing that $u_{n\mathbf{q}}$ are twice differentiable functions of \mathbf{q} , the first and second cumulant moments defined by SWM are:

$$\langle r_\alpha \rangle_c = i \left. \frac{\partial}{\partial k_\alpha} \ln C(\mathbf{k}) \right|_{\mathbf{k}=0}; \quad (\text{A3})$$

$$\langle r_\alpha r_\beta \rangle_c = - \left. \frac{\partial^2}{\partial k_\alpha \partial k_\beta} \ln C(\mathbf{k}) \right|_{\mathbf{k}=0}. \quad (\text{A4})$$

It is immediate to verify that the first cumulant moment is proportional to the macroscopic polarization. Comparing Eq. (A3) to Eq. (22) we immediately get

$$P_\alpha = 2en_b \langle r_\alpha \rangle_c / V_c. \quad (\text{A5})$$

The second cumulant moment derived from the generating function in Eq. (A4) is identical to Eq. (27). To prove this, we start from Eq. (A2): taking two derivatives of the logarithm of S we have

$$\frac{\partial^2}{\partial k_\alpha \partial k_\beta} \ln S = \frac{\partial}{\partial k_\alpha} S^{-1} \frac{\partial}{\partial k_\beta} S + S^{-1} \frac{\partial^2}{\partial k_\alpha \partial k_\beta} S. \quad (\text{A6})$$

We then notice that, to first order in \mathbf{k} ,

$$S^{-1}(\mathbf{q}, \mathbf{q}+\mathbf{k}) \simeq S^\dagger(\mathbf{q}, \mathbf{q}+\mathbf{k}). \quad (\text{A7})$$

replacing Eq. (A7) into Eq. (A6) and taking the trace at $\mathbf{k} = 0$, standard manipulations yield

$$\begin{aligned} & \left. \frac{\partial^2}{\partial k_\alpha \partial k_\beta} \operatorname{tr} \ln S(\mathbf{q}, \mathbf{q}+\mathbf{k}) \right|_{\mathbf{k}=0} \\ &= \sum_{n,n'} \langle u_{n\mathbf{q}} | \frac{\partial}{\partial q_\alpha} u_{n'\mathbf{q}} \rangle \langle \frac{\partial}{\partial q_\beta} u_{n'\mathbf{q}} | u_{n\mathbf{q}} \rangle \\ & \quad - \sum_n \langle \frac{\partial}{\partial q_\alpha} u_{n\mathbf{q}} | \frac{\partial}{\partial q_\beta} u_{n\mathbf{q}} \rangle. \end{aligned} \quad (\text{A8})$$

Using this into Eqs. (A2) and (A4) we get indeed an identical expression to Eq. (27).

One major appeal of the generating function approach of SWM is its very transparent and straightforward discretization. Such discretization leads to the same formulas as found in Sects. III and IV from a different logic. The cumulant generating function, Eq. (A1), is simply discretized on the mesh of Eq. (1) as

$$\ln C(\mathbf{k}) = \frac{1}{n_b M^3} \ln \prod_s \det S(\mathbf{q}_s, \mathbf{q}_s + \mathbf{k}); \quad (\text{A9})$$

we then discretize its \mathbf{k} -derivatives using the same mesh. We have already introduced in Eq. (11) the vector $\Delta \mathbf{q}^{(x)}$ connecting nearest neighbor \mathbf{q} points in the x direction.

Using Eq. (A9), and exploiting the fact that the first derivative is purely imaginary, the first cumulant moment, Eq. (A3), becomes

$$\begin{aligned} \langle x \rangle_c &= -\text{Im} \frac{L}{2\pi} [\ln C(\Delta \mathbf{q}^{(x)}) - \ln C(0)] \\ &= -\frac{a}{2\pi n_b M^2} \text{Im} \ln \prod_s \det S(\mathbf{q}_s, \mathbf{q}_s + \Delta \mathbf{q}^{(x)}). \end{aligned} \quad (\text{A10})$$

Using Eqs. (A5) and (A10) we recover the polarization expression previously reported in Eq. (16).

As for the second cumulant moment, alias localization tensor, we first exploit the reality of the second derivative by writing Eqs. (A4) and (A9) as:

$$\langle r_\alpha r_\beta \rangle_c = -\frac{1}{2} \frac{\partial^2}{\partial k_\alpha \partial k_\beta} \ln |C(\mathbf{k})|^2 \Big|_{\mathbf{k}=0}; \quad (\text{A11})$$

$$\ln |C(\mathbf{k})|^2 = \frac{1}{n_b M^3} \ln \prod_s \det S^\dagger(\mathbf{q}_s, \mathbf{q}_s + \mathbf{k}) S(\mathbf{q}_s, \mathbf{q}_s + \mathbf{k}). \quad (\text{A12})$$

Since the function to be derived is quadratic around $\mathbf{k} = 0$, the discretization is very simple:

$$\begin{aligned} \langle x^2 \rangle_c &= -\frac{1}{|\Delta \mathbf{q}|^2} \ln |C(\Delta \mathbf{q}^{(x)})|^2 \\ &= -\left(\frac{a}{2\pi}\right)^2 \frac{2}{n_b M} \ln \prod_s |\det S(\mathbf{q}_s, \mathbf{q}_s + \Delta \mathbf{q}^{(x)})|, \end{aligned} \quad (\text{A13})$$

and this is indeed identical to Eqs. (24) and (25). We have thus arrived at the same result as first obtained by RS, Eq. (18) therein, providing a more straightforward proof of it.

The expression for the offdiagonal elements of the localization tensor—for a crystal of arbitrary symmetry—is also easily obtained from the SWM formalism. If $f(\mathbf{k})$ is any function quadratic around $\mathbf{k} = 0$, its mixed second derivative is discretized as:

$$\frac{\partial^2 f(0)}{\partial k_\alpha \partial k_\beta} \simeq \frac{1}{|\Delta \mathbf{q}|^2} [f(\Delta \mathbf{q}^{(\alpha)} + \Delta \mathbf{q}^{(\beta)}) - f(\Delta \mathbf{q}^{(\alpha)}) - f(\Delta \mathbf{q}^{(\beta)})], \quad (\text{A14})$$

where $\Delta \mathbf{q}^{(\alpha)}$ is defined in analogy to Eq. (11) for an arbitrary Cartesian direction. Using Eq. (A14) in Eqs. (A11) and (A12) we get:

$$\langle r_\alpha r_\beta \rangle_c = - \left(\frac{a}{2\pi} \right)^2 \frac{1}{2n_b M} \ln \prod_s \frac{|\det S(\mathbf{q}_s, \mathbf{q}_s + \Delta \mathbf{q}^{(\alpha)} + \Delta \mathbf{q}^{(\beta)})|^2}{|\det S(\mathbf{q}_s, \mathbf{q}_s + \Delta \mathbf{q}^{(\alpha)})|^2 |\det S(\mathbf{q}_s, \mathbf{q}_s + \Delta \mathbf{q}^{(\beta)})|^2}. \quad (\text{A15})$$

For the sake of completeness, we also provide the equivalent expression of a typical offdiagonal element in terms of the many-body wavefunction Ψ :

$$\langle xy \rangle_c = - \frac{1}{N} \frac{L^2}{8\pi^2} \ln \frac{|\langle \Psi | e^{i \frac{2\pi}{L} \sum_{i=1}^N (x_i + y_i)} | \Psi \rangle|^2}{|\langle \Psi | e^{i \frac{2\pi}{L} \sum_{i=1}^N x_i} | \Psi \rangle|^2 |\langle \Psi | e^{i \frac{2\pi}{L} \sum_{i=1}^N y_i} | \Psi \rangle|^2}. \quad (\text{A16})$$

In order to evaluate this expression, one needs the expectation value of a slightly more general many-body operator than the one appearing in our basic Eq. (4). An expression similar to Eq. (A16) has explicitly first appeared in Ref. 24.

APPENDIX B: RELATIONSHIP TO BOYS LOCALIZATION IN MOLECULES

We abandon in this Appendix the BvK boundary conditions used throughout this work, and we consider an N -electron system which is bounded in space. Both the orbitals and the many-body wavefunction Ψ are therefore exponentially vanishing at large distances. Supposing that N is even and the state is a singlet, for independent particles the wavefunction is the Slater determinant:

$$\Psi = \frac{1}{N!} |\varphi_1 \bar{\varphi}_1 \varphi_2 \bar{\varphi}_2 \dots \varphi_{N/2} \bar{\varphi}_{N/2}|. \quad (\text{B1})$$

The orbitals enjoy no specific symmetry. Any unitary transformation of the orbitals produces the same many-body ground state (modulo an overall phase): a specific choice of the orbitals will be referred to as “choice of the gauge” in the following. Obviously all ground state

properties are gauge-invariant. The density matrix is twice the projector over the occupied orbitals:

$$\rho(\mathbf{r}, \mathbf{r}') = 2P(\mathbf{r}, \mathbf{r}') = 2 \sum_{i=1}^{N/2} \varphi_i(\mathbf{r}) \varphi_i^*(\mathbf{r}'). \quad (\text{B2})$$

We are interested in exploiting the gauge freedom in order to express the ground state in terms of localized orbitals.¹³ The standard Boys localization¹² in molecules consists in minimizing spherical second moments, in perfect analogy with MV, which can be regarded as the solid-state analogue of Boys localization. Here instead we are mostly interested in localizing in one given direction, say x .

For any given choice of the single-particle orbitals φ_i , the average quadratic spread in the x direction is by definition:

$$\lambda_{xx}^2 = \frac{2}{N} \sum_{i=1}^{N/2} (\langle \varphi_i | x^2 | \varphi_i \rangle - \langle \varphi_i | x | \varphi_i \rangle^2). \quad (\text{B3})$$

We recast this identically as:

$$\begin{aligned} \lambda_{xx}^2 = & \frac{2}{N} \sum_i \langle \varphi_i | x (1 - \sum_j |\varphi_j\rangle \langle \varphi_j|) x | \varphi_i \rangle \\ & + \frac{2}{N} \sum_{i \neq j} |\langle \varphi_i | x | \varphi_j \rangle|^2. \end{aligned} \quad (\text{B4})$$

The first term in Eq. (B4) is gauge invariant, since we can identically write:

$$\lambda_{xx}^2 = \frac{2}{N} \text{Tr } x P x (1 - P) + \frac{2}{N} \sum_{i \neq j} |\langle \varphi_i | x | \varphi_j \rangle|^2, \quad (\text{B5})$$

where “Tr” indicates the trace on the electronic coordinate. The gauge-invariant term in Eq. (B5) can be regarded as the xx element of a more general tensor, which turns out to be the molecular analogue of our localization tensor. We use the same notation for molecules and for crystals:

$$\langle r_\alpha r_\beta \rangle_c = \frac{2}{N} \text{Tr } r_\alpha P r_\beta (1 - P). \quad (\text{B6})$$

If we look for the orbitals which minimize the average spread in the x direction, the solution, after Eq. (B5), is provided by those orbitals which diagonalize the position

operator x , projected over the occupied manifold. Obviously, a set of orthonormal orbitals which diagonalize PxP can always be found, since PxP is a Hermitian operator. The quadratic spread of these orbitals equals $\langle x^2 \rangle_c$, the gauge-invariant part in Eq. (B5). If we are interested instead in minimizing the spherical second moment, in general we *cannot* diagonalize simultaneously PxP , PyP , and PzP . Therefore the spherical spread will be in general *strictly larger* than the Cartesian trace of the localization tensor. This is a key feature in the work of Boys,¹² and MV as well.

We have defined the localization tensor in Eq. (B6). With an obvious generalization of the previous arguments, this tensor provides in general the maximum localizability *in any given direction*. An equivalent expression for the localization tensor is:

$$\langle r_\alpha r_\beta \rangle_c = \frac{1}{N} \int d\mathbf{r} \int d\mathbf{r}' (\mathbf{r} - \mathbf{r}')_\alpha (\mathbf{r} - \mathbf{r}')_\beta |P(\mathbf{r}, \mathbf{r}')|^2, \quad (\text{B7})$$

which has the meaning of the second moment of the (squared) density matrix in the coordinate $\mathbf{r} - \mathbf{r}'$.

At this point, we may think of a crystalline solid as of a very large “molecule”, or a cluster, and take the thermodynamic limit. Since bulk properties must be independent of the choice of boundary conditions (either BvK or “free”), the density matrix and the localization tensor must be the same as the one previously found in this work. And indeed, a glance to Eq. (29) shows that it coincides with the thermodynamic limit of Eq. (B7) in the insulating case. As for the metallic case, our previous findings bear an important message concerning Boys localization. For a cluster of finite size, no matter how large, one can doubtless build localized Boys orbitals. But our results prove that, in the large N limit, the quadratic spread of these Boys orbitals diverges whenever the cluster is metallic.

REFERENCES

- ¹ Permanent address of M. Peressi and R. Resta.
- ² Permanent address of C. Sgiarovello.
- ³ W. Kohn, Phys. Rev. **133**, A171 (1964). See also: W. Kohn, in *Many-Body Physics*, edited by C. DeWitt and R. Balian (Gordon and Breach, New York, 1968), p. 351.
- ⁴ R. Resta, Ferroelectrics **136**, 51 (1992); R.D. King-Smith, and D. Vanderbilt, Phys. Rev. B **47**, 1651 (1993); D. Vanderbilt and R. D. King-Smith, Phys. Rev. B **48**, 4442 (1993); R. Resta, Europhys. Lett. **22**, 133 (1993).
- ⁵ R. Resta, Rev. Mod. Phys. **66**, 899 (1994).
- ⁶ G. Ortíz and R. M. Martin, Phys. Rev. B **43**, 14202 (1994).
- ⁷ R. Resta, Europhysics News **28**, 18 (1997).
- ⁸ R. Resta, Phys. Rev. Lett. **80**, 1800 (1998). See also: R. Resta, Int. J. Quantum. Chem. **75**, 599 (1999).
- ⁹ R. Resta and S. Sorella, Phys. Rev. Lett. **82**, 370 (1999).
- ¹⁰ N. Marzari and D. Vanderbilt, Phys. Rev. B **56**, 12847 (1997).
- ¹¹ I. Souza, T. Wilkens, and R. M. Martin, Phys. Rev. B **62**, 1666 (2000).
- ¹² S.F. Boys, Rev. Mod. Phys. **32**, 296 (1960); J.M. Foster and S.F. Boys, *ibid.* 300.
- ¹³ J. Pipek and P.G. Mezey, J. Chem. Phys. **90**, 4916 (1989).
- ¹⁴ E. I. Blount, in *Solid State Physics*, edited by H. Ehrenreich, F. Seitz and D. Turnbull, vol **13** (Academic, New York, 1962), p. 305.
- ¹⁵ R. Resta, J. Phys.: Condens. Matter **12**, R107 (2000).
- ¹⁶ W. Kohn, Phys. Rev. Lett. **2**, 393 (1959).

- ¹⁷ J. des Cloizeaux, Phys. Rev. **135**, A685 (1964); *ibid.* **135**, A697 (1964).
- ¹⁸ W. Kohn, Phys. Rev. Lett. **76**, 3168 (1996).
- ¹⁹ S. Ismail-Beigi and T.A. Arias, Phys. Rev. Lett. **82**, 2127 (1999).
- ²⁰ W. Jones and N. H. March, *Theoretical Solid State Physics* (Wiley, New York, 1973; reprinted by Dover, New York, 1985).
- ²¹ U. Stephan, R. M. Martin, and D. A. Drabold, Phys. Rev. B **62**, 6885 (2000).
- ²² L. Kleinman and D. M. Bylander, Phys. Rev. Lett. **48**, 1425 (1982); X. Gonze, R. Stumpf, and M. Scheffler, Phys. Rev. B **44**, 8503 (1991).
- ²³ A. Baldereschi, S. Baroni, and R. Resta, Phys. Rev. Lett. **61**, 734 (1988). A complete account can be found in S. Baroni, R. Resta, A. Baldereschi, and M. Peressi, in: *Spectroscopy of semiconductor microstructures*, edited by G. Fasol, A. Fasolino and P. Lugli, NATO ASI Series B, vol 206 (Plenum Publishing, New York, 1989), p 251.
- ²⁴ P. L. Silvestrelli and M. Parrinello, J. Chem. Phys. **111**, 3572 (1999).

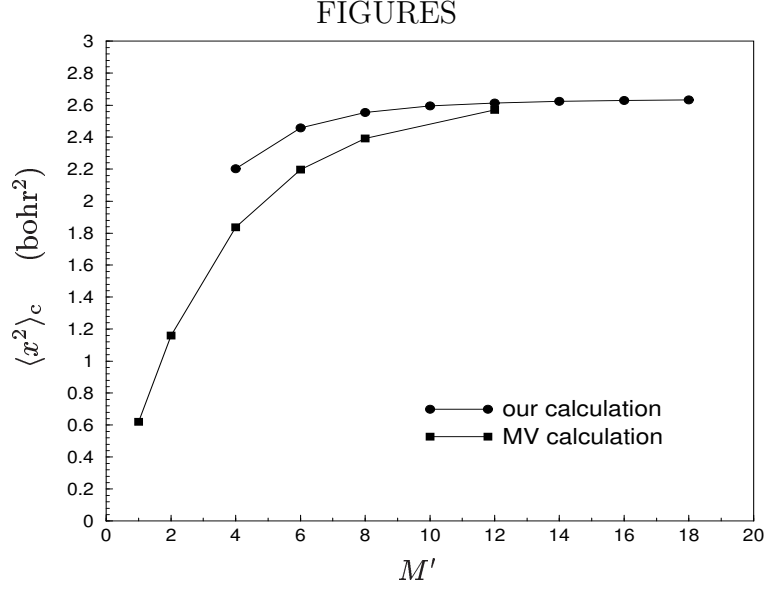


FIG. 1. Convergence of the squared localization length with the size of the sampling grid, for the case of GaAs. We compare our discretized formula with the one used by MV, using a genuinely cubic grid: the label M' means $M' \times M' \times M'$ within MV notations.

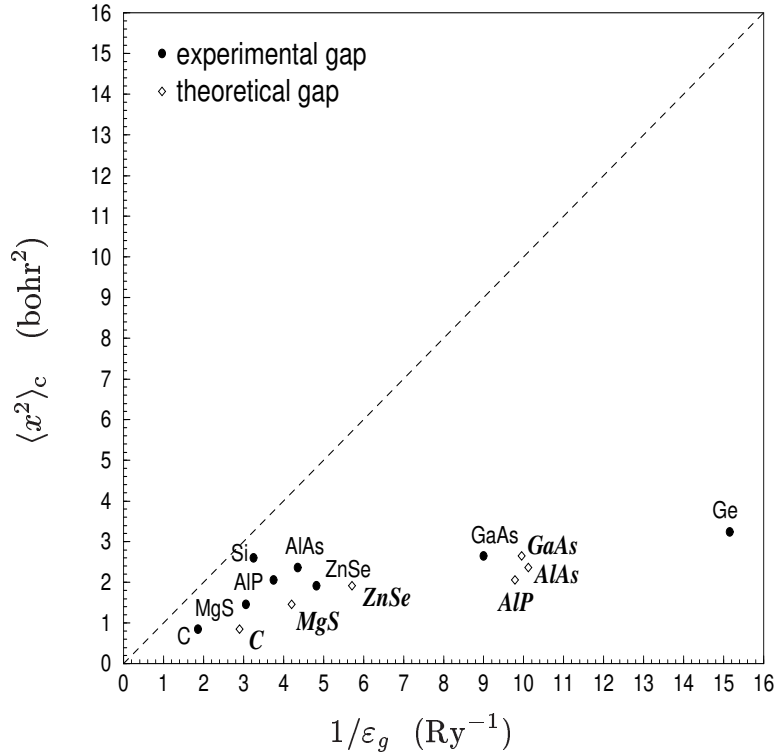


FIG. 2. Squared localization length vs. the inverse direct gap (theoretical and experimental), for several elemental and binary semiconductors. The inequality of Eq. (34) is strongly verified. The points corresponding to Si and Ge with the theoretical gaps are out of scale.

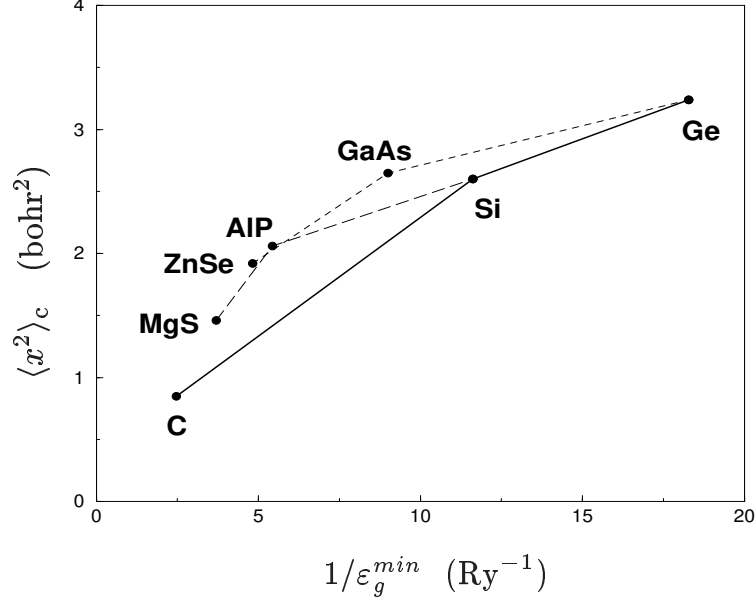


FIG. 3. Trends of the squared localization length vs. the inverse experimental minimum gap. The lines connect the isoelectronic series MgS–AlP–Si and ZnSe–GaAs–Ge, and the isovalent one C–Si–Ge.

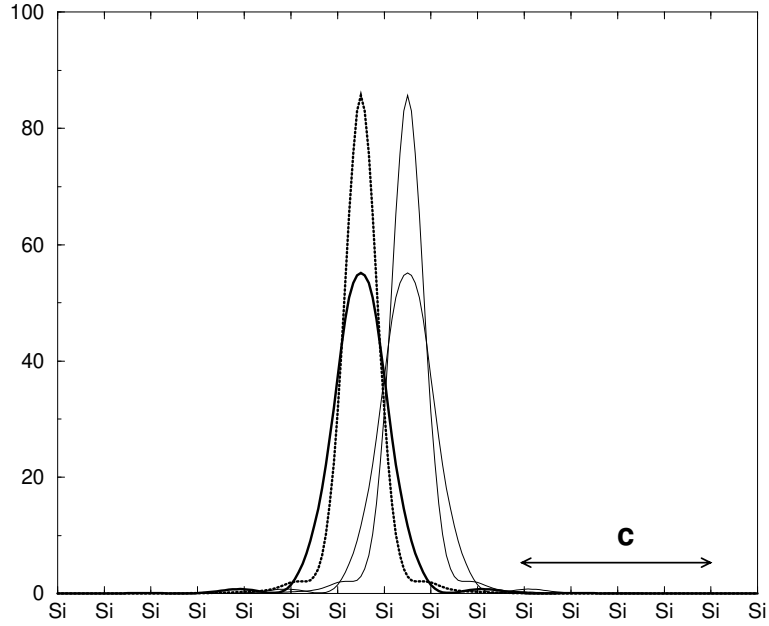


FIG. 4. Hermaphrodite orbitals for Si. The quantity displayed is $n_{loc}(x)$, defined as the xy average of the square modulus of the orbital w_{j,s_2,s_3} , for $s_2 = s_3 = 0$, and for the four j values localizing within the same cell.

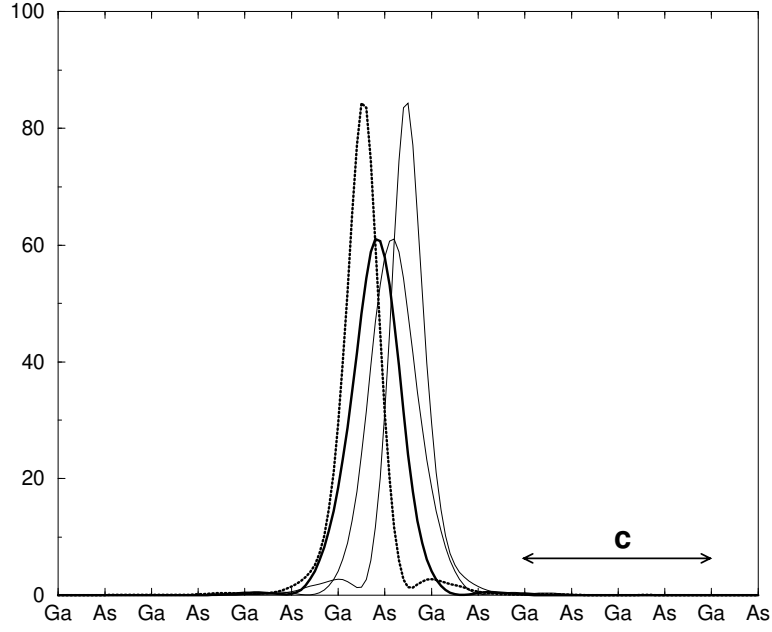


FIG. 5. Hermaphrodite orbitals for GaAs. The quantity displayed is $n_{\text{loc}}(x)$, defined as the xy average of the square modulus of the orbital w_{j,s_2,s_3} , for $s_2 = s_3 = 0$, and for the four j values localizing within the same cell.

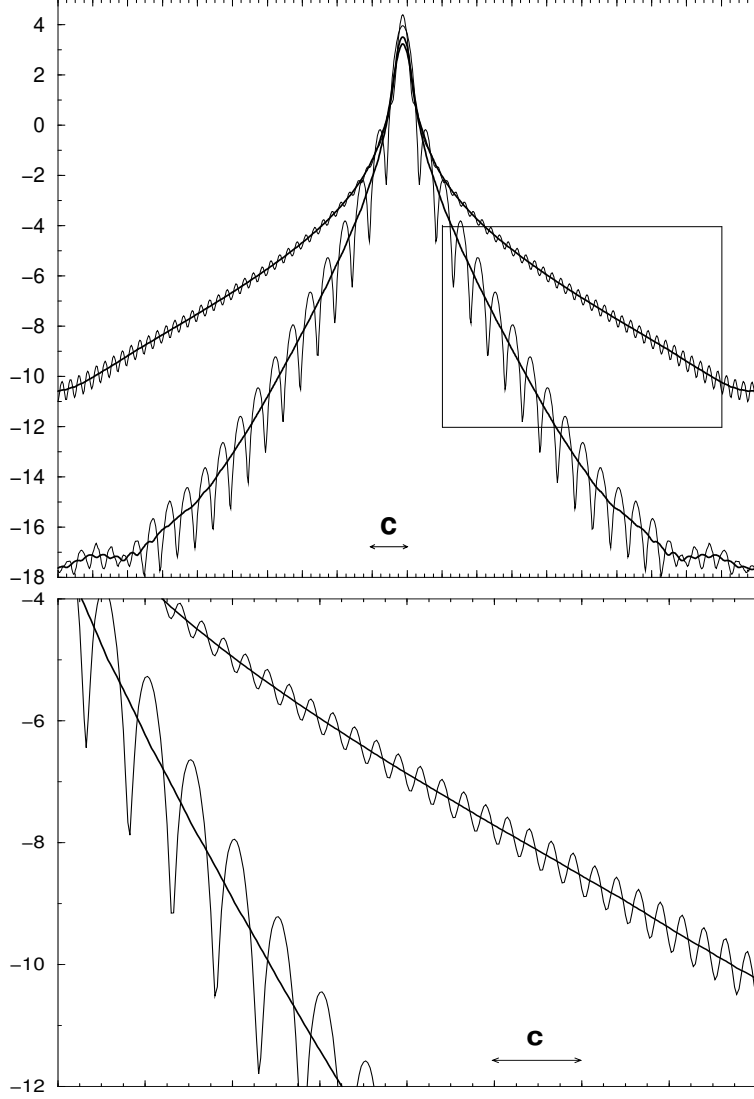


FIG. 6. Exponential decay of two hermaphrodite orbitals for Ge. Thin lines correspond to the logarithm of two different $n_{\text{loc}}(x)$, defined as the xy average of the square modulus of the orbital w_{j,s_2,s_3} , for the same j and two different points of the two-dimensional mesh(s_2,s_3). The one with the slowest decay corresponds to $s_2 = s_3 = 0$. Thick lines are the macroscopic average (see text) of $\ln n_{\text{loc}}(x)$. The lower panel is a magnification of the region indicated in the upper panel in order to better appreciate the linear behavior of $\ln n_{\text{loc}}(x)$.

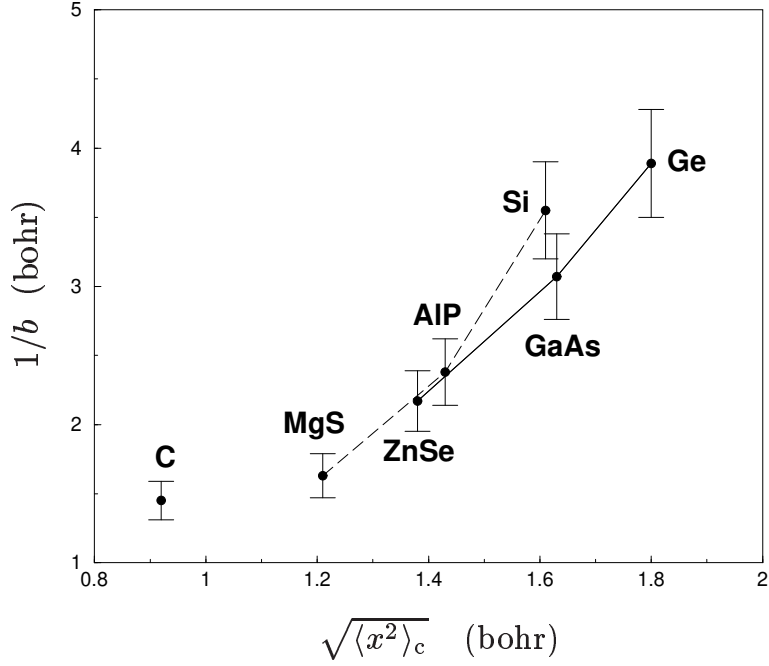


FIG. 7. Exponential decay length, averaged over the two-dimensional mesh (s_2, s_3) , vs. our localization length (square root of the second cumulant moment). The straight-line segments are only a guide to the eye linking compounds of the same isoelectronic series. The vertical bars are an estimate of the accuracy of the interpolation scheme used to extract the b value from the asymptotic macroscopic average of $n_{\text{loc}}(x)$.